

Articles

A New Chiral at Metal Catalyst for Enantioselective Diels–Alder Reactions: Observation of Isomeric Intermediates

J. W. Faller* and Brian J. Grimmond

Department of Chemistry, Yale University, New Haven, Connecticut 06520

Received December 18, 2000

The chiral at metal complex [CyRuCl(*R*)-QUINAP]SbF₆, **1**, was prepared from (CyRuCl₂)₂, (*R*)-QUINAP, and AgSbF₆. Characterization by ¹H, ³¹P{¹H}, and ¹³C{¹H} NMR spectroscopy indicated a 5:1 mixture of diastereomers was present; single-crystal X-ray diffraction studies revealed that the major diastereomer possessed the (*R*_{Ru}, *R*_{QUINAP}) absolute configuration. The dicationic complex, which was prepared in situ when **1** was treated with 0.9 equiv of AgSbF₆, catalyzed the Diels–Alder reaction of CpH and methacrolein in 99% ee at –24 °C.

Introduction

Chiral complexes of transition metals¹ and main group metalloids² are becoming increasingly popular as catalysts for fundamental asymmetric C–C bond forming reactions. In the transition metal-containing catalysts, a Lewis acidic metal is often bound by a chiral C₂-symmetric ligand. The metal functions as a docking site which binds and activates an organic substrate toward Diels–Alder reactions, for example. The result is a preferential orientation of the substrate which results in the enantiomeric purity of the product being controlled by the chiral ligand.

We have explored the chemistry of cationic chiral at metal complexes and sought to investigate their ability as Lewis acid catalysts for stereoselective Diels–Alder reactions.³ Of particular interest was the possibility that stereocontrol of the product could be augmented by the direct interaction of a stereogenic metal center with a bound reactant. Recent contributions have described the stereoselective synthesis of such systems with encouraging applications to catalytic enantioselective organic transformations.^{1d,4} Reported here is the facile synthesis and characterization of the novel complex [CyRuCl(*R*)-

QUINAP]SbF₆, **1** (Cy = *p*-cymene, QUINAP = 1-(2-diphenylphosphino-1-naphthyl)isoquinoline), and preliminary data obtained when using a catalyst, which was derived from **1** and prepared in situ, for the Diels–Alder reaction between CpH (CpH = cyclopentadiene) and α -substituted acroleins.

Results and Discussion

Compound **1** was readily synthesized by a salt metathesis route (Scheme 1) in good yield (77%) and was isolated as an air-stable orange solid. Characterization by NMR spectroscopy revealed that **1** contained a 5:1 mixture of diastereomers. ³¹P{¹H}: δ 26.0 (s) major/47.6 (s) minor. Proton NMR indicated that there was partial inclusion of CH₂Cl₂. Recrystallization from CH₂Cl₂/Et₂O provided fine orange needles of **1**, whereas a CHCl₃/Et₂O recrystallization afforded crystals suitable for X-ray diffraction studies. A crystalline sample of exclusively the major diastereomer was obtained from the crude reaction mixture upon repeated recrystallization from CHCl₃/Et₂O. This was established via analysis of this crystalline sample by ³¹P{¹H} NMR spectroscopy, where a single ³¹P resonance at δ 26 was observed indicating the presence of only one diastereomer in the bulk sample. The solid-state structure of **1** (Figure 1) indicated that the major diastereomer possessed the (*R*_{Ru}, *R*_{QUINAP}) configuration, the minor diastereomer therefore being the (*S*_{Ru}, *R*_{QUINAP}) epimer. For chirality description purposes,⁵ the Ru center can be viewed as

(1) (a) Kündig, E. P.; Saudan, C. M.; Bernardinelli, G. *Angew. Chem., Int. Ed.* **1999**, *38*, 1220. (b) Jørgensen, K. A.; Johannsen, M.; Yoa, S.; Audrain, H.; Thorhauge, J. *Acc. Chem. Res.* **1999**, *32*, 605. (c) Bruin, M. E.; Kündig, E. P. *Chem. Commun.* **1998**, 2635. (d) Davenport, A. J.; Davies, D. L.; Fawcett, J.; Garratt, S. A.; Lad, L.; Russell, D. R. *Chem. Commun.* **1997**, 2347. (e) Kündig, E. P.; Bourdin, B.; Bernadelli, G. *Angew. Chem., Int. Ed. Engl.* **1994**, *33*, 1856. (f) Kagan, H. B.; Riant, O. *Chem. Rev.* **1992**, *92*, 1007.

(2) (a) Corey, E. J.; Guzman-Perez, A. *Angew. Chem., Int. Ed.* **1998**, *37*, 388. (b) Ishihara, K.; Kurihara, H.; Matsumoto, M.; Yamamoto, H. *J. Am. Chem. Soc.* **1998**, *120*, 6920. (c) Furuta, K.; Shimizu, S.; Miwa, Y.; Yamamoto, H. *J. Org. Chem.* **1989**, *54*, 1481. (d) Hashimoto, S.; Komeshima, N.; Koga, K. *Chem. Commun.* **1979**, 437.

(3) (a) Faller, J. W.; Parr, J. *Organometallics* **2000**, *19*, 1829. (b) Faller, J. W.; Liu, X.; Parr, J. *Chirality* **2000**, *12*, 325. (c) Faller, J. W.; Patel, B. P.; Albrizzio, M. A.; Curtis, M. *Organometallics* **1999**, *18*, 3096. (d) Faller, J. W.; Lavoie, A., *J. Organometal Chem.* **2001**, in press.

(4) Therien, B.; Ward, T. *Angew. Chem., Int. Ed.* **1999**, *38*, 405. (b) Davies, D. L.; Fawcett, J.; Garratt, S. A.; Russell, D. R. *Chem. Commun.* **1997**, 1351. (c) Carmona, D.; Cativiela, C.; Elipe, S.; Lahoz, F. J.; Lamata, M. P.; López-Ram du Viu, M. P.; Oro, L. A.; Vega, C.; Viguri, F. *Chem. Commun.* **1997**, 2351. (d) Carmona, D.; Cativiela, C.; García-Correas, R.; Lahoz, F. J.; Lamata, M. P.; López, J. A.; López-Ram du Viu, M. P.; Oro, L. A.; Emilio, S. J.; Viguri, F. *Chem. Commun.* **1996**, 1247.

(5) Stanley, K.; Baird, M. C. *J. Am. Chem. Soc.* **1975**, *97*, 6598.

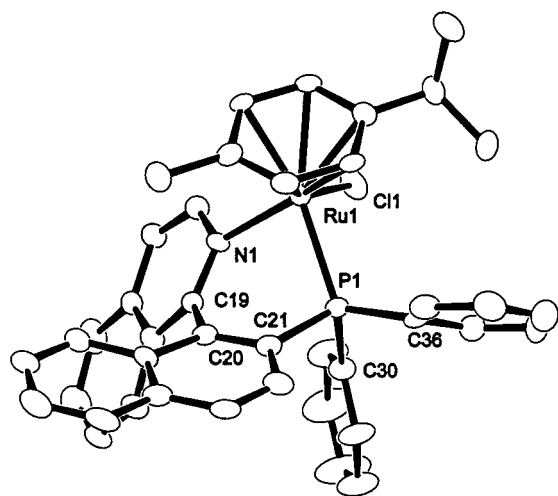
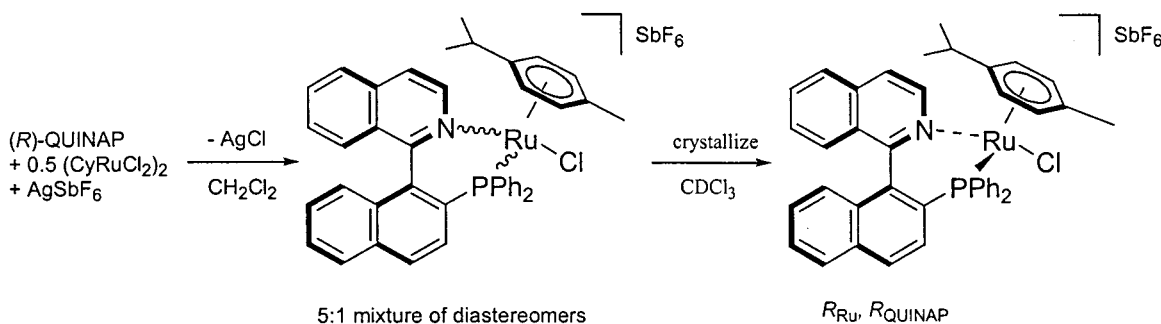
Scheme 1. Preparation and Resolution of **1**

Figure 1. ORTEP diagram of the cation in (R_{Ru}, R_{QUINAP}) - $[CyRuCl(QUINAP)]SbF_6 \cdot CHCl_3$, **1**, showing 50% probability ellipsoids.

pseudo-tetrahedral if one considers the metal binding to the Cy centroid. Significantly, the (R) -QUINAP ligand was oriented such that the PPh_2 phenyl rings are projected toward the chloride ligand, partly shielding the Ru–Cl bond. It is, therefore, probable that the approach of a reagent to the metal center would occur from the quadrant occupied by the isoquinoline-based ligand rather than from the diarylphosphine. The P(1)–Ru–N(1) bite angle of 82.0° was similar to other six-membered chelate rings of other arene ruthenium systems containing heterobidentate ligands.^{3,6} The dihedral angle between the naphthyl rings was $56.1(9)^\circ$, which is somewhat smaller than typically observed in related metal complexes of C_2 -symmetric chelating ligands such as BINAP.

Salt metathesis with 0.9 equiv of $AgSbF_6$ converted **1** to the corresponding aqua species $[CyRu(OH_2)(R)QUINAP](SbF_6)_2$, **2**, which was an active catalyst for the Diels–Alder reaction of CpH and α -substituted enals. The formation of aqua species from moisture in the solvent has been frequently observed.⁷ An excess of **1** was used in catalytic reactions because it was essential

Table 1. Lewis Acid-Catalyzed Diels–Alder Reactions of CpH with $[CyRu(H_2O)(R)QUINAP](SbF_6)_2$

entry	(R)	catalyst ^a loading (%)	temp (°C)	conversion ^b (%)	de ^c (%)	ee ^d (%) [config.]
1	(Me)	10	−78	100	95	50 [<i>S</i> (+)]
2	(Me)	10	−24	100	91	99 [<i>S</i> (+)]
3	(Et)	10	−78	100	96	32
4	(Et)	10	−24	100	97	51

^a All reactions were conducted in CH_2Cl_2 with the Lewis acid generated in situ from $[CyRuCl(R)QUINAP]SbF_6$ (11 mol %) and $AgSbF_6$ (10 mol %). ^b Conversion of the acroleins to the corresponding DA product was determined by 1H NMR analysis of the crude reaction mixture. ^c The de was determined by 1H NMR spectroscopy on integration of the *exo* and *endo* aldehyde proton resonances. The de refers to the excess of the *exo* diastereomer. ^d The resonances for the enantiomers from **1** and **2** were resolved by 1H NMR spectroscopy using the chiral shift reagent $Eu(hfc)_3$, and the ee was then determined using the line shape deconvolution program Peak Fit 4.0. The absolute configuration of the product was established by comparison of the specific rotation to the literature values.

to ensure that there was virtually no free $AgSbF_6$ in solution that could act as a competitive catalyst and would yield racemic product. The cycloadditions of CpH to methacrolein and ethacrolein were investigated at temperatures of -78 and -24 °C (Table 1). With a catalyst loading of 10 mol % the reaction times at -24 °C were approximately 2 h, as established by 1H NMR spectroscopy, although the solutions were generally allowed to stand for 12 h to ensure reaction completion. The crude reaction mixture was typically added to pentanes, precipitating the catalyst, which could then be readily separated upon filtration through Celite. The isolated catalyst residue was an air-stable orange solid, which was analyzed by $^{31}P\{^1H\}$ NMR spectroscopy. This revealed that the H_2O adduct, **2**, and a small amount of the chloride precursor, **1**, were present, indicating that the catalyst complex remained intact and, in principle, could be recycled upon workup.

In all cases, the catalyst demonstrated good *exo*-cycloadduct diastereoselectivity; the de ranged from 91 to 97%. With regard to enantioselectivity, *exo*-2-ethylbicyclo[2.2.1]hept-5-ene-2-carboxaldehyde (entries 1, 2) was obtained with moderate ee (51%), although *exo*-2-methylbicyclo[2.2.1]hept-5-ene-2-carboxaldehyde (entries 3, 4) could be isolated with excellent (*S*)-enantioselectivity (99%) when the reaction was performed at -24 °C. This marks one of the few cases where a complex containing a stereogenic metal center has achieved high enantioselectivity as a catalyst for the Diels–Alder reaction of an acrolein and CpH. Somewhat surprisingly, it was also noted that the level of enantio-

(6) Faller, J. W.; Grimmond, B. J.; Curtis, M. C. *Organometallics* **2000**, *19*, 5174.

(7) Aqua complexes are frequently observed in nonpolar solvents of organometallic Lewis acids.⁴ Some specific examples are with (a) Cp^*Rh : Carmona, D.; Cativiela, C.; Garcia-Correas, R.; Lahoz, F. J.; Lamata, M. P.; Lopez, J. A.; Viu, M. P. L.-R.; Oro, L. A.; Jose, E. S.; Viguri, F. J. *Chem. Soc., Chem. Commun.* **1996**, 1247. (b) $Tp(i-Pr)Ru$: Takahashi, Y.; Akita, M.; Hikichi, S.; Moro-oka, Y. *Inorg. Chem.* **1998**, *37*, 3186. (c) $Tp(i-Pr)Ru$: Takahashi, Y.; Hikichi, S.; Akita, M.; Moro-oka, Y. *Chem. Commun.* **1999**, 1491. (d) $(PAN)Ru$.^{4a}

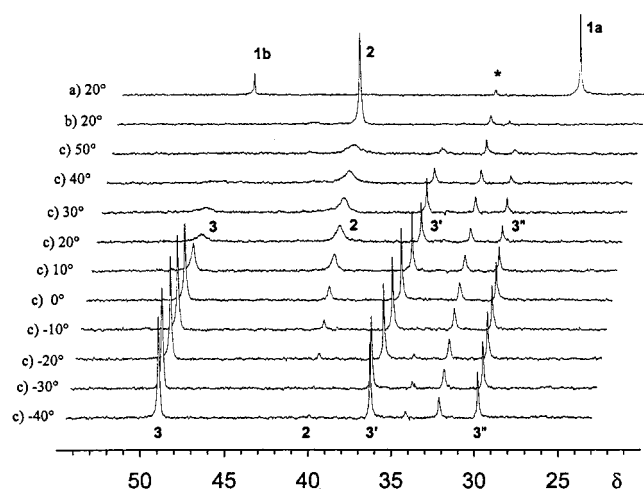


Figure 2. Variable-temperature $^{31}\text{P}\{^1\text{H}\}$ NMR stack plot of the components of the catalyst mixture: (a) $[\text{CyRuCl}(R)\text{-QUINAP}](\text{SbF}_6)_2$; (b) $[\text{CyRu}(\text{OH}_2)(R)\text{-QUINAP}](\text{SbF}_6)_2$; (c) $[\text{CyRu}(\text{OH}_2)(R)\text{-QUINAP}](\text{SbF}_6)_2 + \text{methacrolein}$. Temperatures in $^\circ\text{C}$. * denotes an impurity (see Supporting Information for spectra free of the impurity).

selectivity dropped substantially for both dieneophiles when the reaction was carried out at -78°C .

The in-situ prepared catalyst, **2**, was monitored with and without methacrolein by VT NMR spectroscopy as a possible means to determine the source of the observed temperature-dependent variation in enantioselectivity. A methylene chloride- d_2 solution of **1** (5:1 mixture of diastereomers) was allowed to react with AgSbF_6 to provide the proposed aqua species $[\text{CyRu}(\text{OH}_2)(R)\text{-QUINAP}](\text{SbF}_6)_2$, **2**. The $^{31}\text{P}\{^1\text{H}\}$ NMR spectrum (Figure 2) revealed that a single diastereomer of **2** (δ 39) was present; cooling from 20°C to -80°C in increments of 20°C did not result in significant line broadening or in the evolution of further resonances. This suggested that the aqua complex existed as a single diastereomer throughout the temperature range examined.

When an excess of methacrolein (~ 10 equiv) was added to a solution of **2**, however, four signals were observed in a ratio of 2.2:4.1:2.2:1.0 by $^{31}\text{P}\{^1\text{H}\}$ NMR spectroscopy at 20°C (Figure 2).⁸ A broad resonance (δ 39, relative intensity 4.1) was assigned to the aqua compound **2** on the basis of chemical shift, whereas the three new resonances (δ 49, 35, 28 in a 2.2:2.2:1.0 ratio) were assigned to isomers of the methacrolein complex $[\text{CyRu}\cdot\text{methacrolein}\text{-}(R)\text{-QUINAP}](\text{SbF}_6)_2$, **3**, **3'**, and **3''** respectively. The methacrolein isomer detected at δ 49, **3**, was broad at ambient temperature owing to rapid exchange, whereas the remaining resonances, **3'** and **3''**, did not show significant line broadening due to exchange until the solution was heated. A series of $^{31}\text{P}\{^1\text{H}\}$ spin saturation transfer experiments at 20°C unambiguously confirmed that the aqua complex **2** exchanged with **3**, but also with **3'** and **3''**. The $^{31}\text{P}\{^1\text{H}\}$ VT NMR analysis of this solution provided the activation energies

(8) The intensity of the resonance for aqua compound **2** increased with decreasing concentration of methacrolein. The NMR experiments on the catalyst solution of $[\text{CyRu}(\text{methacrolein})(R)\text{-QUINAP}](\text{SbF}_6)_2$, **3**, **3'**, and **3''** were repeated numerous times. An additional peak (δ 31) was occasionally detected and is assigned to the product of partial catalyst decomposition. This assignment was made on the basis of VT NMR and SST experiments, which demonstrated that this compound was not involved in the exchange processes observed for **2**, **3**, **3'**, and **3''**.

of exchange for each methacrolein isomer as $\Delta G^\ddagger = 14.3$ $\text{kcal}\cdot\text{mol}^{-1}$ (**3**, $T_1 = -10^\circ\text{C}$), 16.3 $\text{kcal}\cdot\text{mol}^{-1}$ (**3'**, $T_1 = 20^\circ\text{C}$), and 17.0 $\text{kcal}\cdot\text{mol}^{-1}$ (**3''**, $T_1 = 30^\circ\text{C}$).⁹ When monitored against an internal standard the VT experiments indicated that, on cooling, the intensity of the resonances for **3**, **3'**, and **3''** increased while that of aqua complex **2** decreased. Furthermore, when cooled below -40°C , virtually all of complex **2** was converted to the methacrolein complexes (**3**:**3'**:**3''** ratio of 2.4:1.4:1.0) with **3** present as the dominant species. Further cooling (below -78°C) did not significantly alter the ratio of the methacrolein complexes.

It is likely that the complex behavior of the catalyst solution with temperature contributes to the temperature-dependent ee of the Diels–Alder cycloadduct. This mixture of potential catalysts could produce variations in overall enantioselectivity for a given Diels–Alder cycloadduct depending on which enal π -diastereoface was exposed within each active catalyst isomer. Although the exact nature of the isomeric Ru-methacrolein adducts **3**, **3'**, and **3''** could not be deduced, it is likely that two epimers, i.e., (S_{Ru} , R_{QUINAP}) and (R_{Ru} , R_{QUINAP}), in addition to another conformer of one epimer were observed by $^{31}\text{P}\{^1\text{H}\}$ NMR spectroscopy.¹⁰ The ratio of these components did not vary significantly between -24 and -78°C , suggesting that any strong variation in overall catalyst enantioselectivity was dependent on their relative catalytic activities rather than simply on the proportion of each catalyst complex. It is proposed that, at -24°C , the differences in catalytic activity of the methacrolein complexes **3**, **3'**, and **3''** with CpH were significantly different. In this manner one or more ruthenium species produced predominantly the same enantiomer of the Diels–Alder adduct. This resulted in excellent methacrolein diastereofacial discrimination on reaction with CpH, affording *exo*-2-methylbicyclo[2.2.1]-hept-5-ene-2-carboxaldehyde with high enantioselectivity [99%-(*S*)]. However, when cooled to -78°C , a second distribution of catalytic activities (rates) for **3**, **3'**, and **3''** was obtained. Under these conditions, at least two Ru-methacrolein adducts provided opposite enantiomers of the cycloadduct at competitive rates of catalytic activity. This would then account for the observed drop in enantioselectivity [50% (*S*)] between the temperatures of -24 and -78°C . It is also possible that the decrease in catalytic activity of the Ru species at lower temperatures allowed other achiral acid sources in the reaction mixture to compete with the chiral Lewis acid catalyst, thereby reducing the enantiomeric purity of the Diels–Alder product.

Conclusion

In conclusion, the new compound $[\text{CyRuCl}(R)\text{-QUINAP}](\text{SbF}_6)_2$, **1**, has been readily synthesized and characterized by standard methods. When treated with AgSbF_6 , the resulting ruthenium complex catalyzed the Diels–Alder reaction of CpH and methacrolein with excellent enantioselectivity [99%-(*S*)] at -24°C . The

(9) Faller, J. W. In *Encyclopedia of Inorganic Chemistry*; King, R. B., Ed.; John Wiley and Sons: New York, 1994; p 3914.

(10) The η^2 -coordination of aldehydes to cationic rhenium centers has also been well documented: Gladysz, J. A.; Boone, B. J. *Angew. Chem., Int. Ed. Engl.* **1997**, *36*, 550. In this case, conformational isomers probably arise from orientations of the cymene.

decrease in ee at $-78\text{ }^{\circ}\text{C}$ [50%-(S)] was attributed in part to significant changes in the relative catalytic activity of isomers of the methacrolein complexes **3**, **3'**, and **3''** which were observed by $^{31}\text{P}\{^1\text{H}\}$ NMR spectroscopy.

Experimental Section

All synthetic manipulations were carried out using standard Schlenk techniques under an inert atmosphere. The ligand (*R*)-QUINAP was purchased from Strem Chemical and was used without further purification. A synthesis of (CyRuCl)₂ has been published.¹¹ The enantiomeric excess in the methacrolein product was determined by addition of the chiral shift reagent europium tris[3-(heptafluoropropylhydroxymethylene)-(+)-camphorate] (98%) to an aliquot of Diels–Alder product in CDCl₃. The absolute configuration of the methacrolein Diels–Alder adduct was assigned on the basis of comparison of optical rotation.¹² The enantiomeric purity of the ethacrolein adduct was determined by NMR after derivitization with (2*R*,4*R*)-pentanediol. ^1H NMR spectra were recorded on a Bruker 500 MHz (shift reagent experiments) or Bruker 400 MHz spectrometer, and chemical shifts are reported in ppm relative to residual solvent peaks (^1H). Elemental analyses were performed by Atlantic Microlab, Inc., Norcross, GA.

Synthesis of [CyRuCl(*R*)-QUINAP]SbF₆. In a glovebox, a Schlenk tube was charged with (CyRuCl₂)₂ (0.036 g, 0.058 mmol) and (*R*)-QUINAP (0.050 g, 0.120 mmol). The vessel was then transferred to a Schlenk line, where it was evacuated and backfilled with N₂. A sample of CH₂Cl₂ (15 mL) was vacuum transferred to the vessel, and the reaction mixture was then allowed to warm to ambient temperature under vacuum. The degassed solution was then stirred for 0.5 h to provide an orange solution. A sample of AgSbF₆ (0.040 g, 0.12 mmol) was added under a stream of N₂, and the resulting cloudy orange solution was stirred for 24 h. The reaction mixture was filtered through Celite to give a clear orange solution, from which the volatiles were removed in vacuo. The resulting orange powder was dried in vacuo for 1 h to give **1** (0.100 g, 77% yield) as a 5:1 mixture of diastereomers. Major diastereomer: $^{31}\text{P}\{^1\text{H}\}$ NMR (162 MHz, CDCl₃, 298 K): 26.0 (s). ^1H NMR (400 MHz, CDCl₃, 298 K): 9.53 (d, $J = 6.6$ Hz, 1 H, iso-*H*), 8.46 (m, 2 H, Ar-*H*), 8.10 (d, $J = 8.2$ Hz, 1 H, Ar-*H*) 7.97–6.57 (m, Ar-*H*), 5.62 (d, $J = 6.5$ Hz, 1 H, Cy-*H*) 5.55 (d, $J = 6.5$ Hz, 1 H, Cy-*H*), 5.46 (d, $J = 5.8$ Hz, 1 H, Cy-*H*) 4.81 (d, $J = 5.8$ Hz, 1 H, Cy-*H*), 2.46 (spt, $J = 7.0$ Hz, 1 H, Cy CHMe), 1.22 (s, 3 H, Cy CH₃), 1.07 (d, $J = 7.0$ Hz, 3 H, Cy CHCH₃), 0.73 (d, $J = 7.0$ Hz, 3 H, Cy CHCH₃). Minor diastereomer: $^{31}\text{P}\{^1\text{H}\}$ NMR (162 MHz, CDCl₃, 298 K): 47.7 (s). ^1H NMR (400 MHz, CDCl₃, 298 K): 9.43 (d, $J = 6.6$ Hz, 1 H, iso-*H*), 7.97–6.57 (m, Ar-*H*), 6.52 (d, $J = 6.5$ Hz, 1 H, Cy-*H*), 5.97 (d, $J = 5.8$ Hz, 1 H, Cy-*H*), 5.21 (d, $J = 6.6$ Hz, 1 H, Cy-*H*), 3.14 (spt, $J = 7.0$ Hz, 1 H, Cy CHMe), 1.99 (s, 3 H, Cy CH₃), 1.47 (d, $J = 7.0$ Hz, 3 H, Cy CHCH₃), 1.31 (d, $J = 7.0$ Hz, 3 H, Cy CHCH₃). $^{13}\text{C}\{^1\text{H}\}$ NMR (100 MHz, CDCl₃, 298 K) 5:1 mixture of diastereomers: 161.24, 161.11, 149.43, 139.35, 139.21, 136.49, 136.25, 136.05, 134.27, 134.05, 133.96, 133.85, 133.78, 133.75, 133.71, 133.69, 132.76, 132.48, 132.45, 132.41, 130.52, 130.19, 130.03, 129.97, 129.93, 129.56, 129.49, 129.13, 128.98, 128.87, 128.76, 128.69, 128.52, 128.44, 128.21, 127.93, 127.60, 127.50, 127.00, 126.92, 126.26, 125.66, 124.22, 123.18, 122.82, 122.79, 109.77, 109.76, 102.13, 101.47, 95.91, 95.84, 91.97, 91.90, 88.21, 88.18, 85.52, 31.24, 30.66, 23.84, 23.38, 20.17, 19.95, 19.34, 18.74. Major diastereomer: 149.43, 134.05, 133.96, 133.85, 133.78, 132.76, 132.45, 130.52, 130.03, 129.93, 129.56, 128.76, 128.69, 128.52, 128.44, 127.60, 127.50, 127.00, 125.66,

Table 2. Crystallographic Data for X-ray Diffraction Study of (*R*_{Ru},*R*_{QUINAP})-[CyRuCl(QUINAP)]SbF₆·CHCl₃, **1'**

formula	SbRuCl ₃ PF ₆ NC ₄₁ H ₃₇ ·CHCl ₃
cryst syst	monoclinic
space group	<i>P</i> 2 ₁ (No. 4)
<i>a</i> , Å	13.8092(6)
<i>b</i> , Å	11.1318(4)
<i>c</i> , Å	15.0703(5) Å
β , deg	113.450(2)
<i>V</i> , Å ³	2125.3(1)
<i>fw</i>	1066.37
ρ_{calcd} , g/cm ³	1.666 (<i>Z</i> = 2)
abs coeff (cm ⁻¹)	13.37
cryst size, mm	0.05 × 0.07 × 0.22
diffractometer	Nonius KappaCCD
monochromator	graphite
radiatn	Mo K α (0.71073 Å)
max 2θ , deg	55.0
data images	94 exposures @ 150 s
ω oscillation range, deg	2.0
detector position	35 mm
no. of reflns measd	total: 11849
	unique: 5113 (<i>R</i> _{int} = 0.037)
data used, $F^2 > 3\sigma(F^2)$	4111
no. of params refined	504
<i>p</i> factor	0.01
final residuals <i>R</i> , <i>R</i> _w	0.039, 0.040
convergence, largest shift/error	0.00
GOF	1.34
largest $\Delta(\rho)$ (e Å ⁻³)	0.58

Table 3. Selected Bond Distances (Å) and Angles (deg) for (*R*_{Ru},*R*_{QUINAP})-[CyRuCl(QUINAP)]SbF₆·CHCl₃, **1'**

Ru(1)	Cl(1)	2.401(2)		Ru(1)	P(1)	2.332(2)	
Ru(1)	N(1)	2.131(5)					
Cl(1)	Ru(1)	N(1)	87.8(1)	Cl(1)	Ru(1)	P(1)	90.7(1)
P(1)	Ru(1)	N(1)	82.0(1)				

123.18, 122.79, 109.76, 101.47, 95.91, 91.97, 88.18, 85.52, 30.66, 23.38, 19.94, 18.74. Anal. Calcd for C₄₁H₃₆ClF₆NPRuSb·0.5(CH₂Cl₂): C, 50.43; H, 3.77; N, 1.42. Found: C, 50.53; H, 4.30; N, 1.47.

Fractional Crystallization of [CyRuCl(*R*)-QUINAP]SbF₆. Recrystallization of a 5:1 mixture of diastereomers from CH₂Cl₂/Et₂O (1:2) at ambient temperature provided orange needles of **1**. The needles were then isolated from the mother liquor and recrystallized from CHCl₃/Et₂O (1:2) at ambient temperature to afford orange crystals of **1'**, which contain CHCl₃ in the lattice and were suitable for X-ray diffraction. When the solid-state structure was found to correspond exclusively to the (*R*_{Ru}, *R*_{QUINAP}) diastereomer, the remaining crop of crystals was dissolved in CDCl₃ and examined by ^1H and $^{31}\text{P}\{^1\text{H}\}$ NMR spectroscopy. The solution-state study indicated that a single diastereomer, which corresponded to the major diastereomer of the crude reaction mixture, was present. (*R*_{Ru}, *R*_{QUINAP})-**1** $^{31}\text{P}\{^1\text{H}\}$ NMR (162 MHz, CDCl₃, 298 K): 26.0 (s). ^1H NMR (400 MHz, CDCl₃, 298 K): 9.53 (d, $J = 6.6$ Hz, 1 H, Ar-*H*), 8.47 (d, $J = 5.0$ Hz, 1 H, Ar-*H*), 8.13 (d, $J = 8.3$ Hz, 1 H, Ar-*H*), 7.99 (d, $J = 7.9$ Hz, 1 H, Ar-*H*), 7.96 (d, $J = 7.9$ Hz, 1 H, Ar-*H*), 7.82 (d, $J = 8.3$ Hz, 1 H, Ar-*H*), 7.78 (d, $J = 6.6$ Hz, 1 H, Ar-*H*), 7.73–7.57 (m, 5 H, Ar-*H*), 7.35–7.25 (m, Ar-*H*), 7.13 (app t, $J = 7.8$ Hz, Ar-*H*), 6.89 (d, $J = 9.0$ Hz, 1 H, Ar-*H*), 6.75 (m, 1 H, Ar-*H*), 6.65 (d, $J = 8.9$ Hz, 1 H, Ar-*H*), 6.60 (td, $J = 7.7$, 3.0 Hz, 2 H, Ar-*H*), 5.62 (d, $J = 6.5$ Hz, 1 H, Cy-*H*) 5.55 (d, $J = 6.5$ Hz, 1 H, Cy-*H*), 5.46 (d, $J = 5.8$ Hz, 1 H, Cy-*H*) 4.81 (d, $J = 5.8$ Hz, 1 H, Cy-*H*), 2.46 (spt, $J = 7.0$ Hz, 1 H, Cy CHMe), 1.22 (s, 3 H, Cy CH₃), 1.07 (d, $J = 7.0$ Hz, 3 H, Cy CHCH₃), 0.73 (d, $J = 7.0$ Hz, 3 H, Cy CHCH₃).

X-ray Crystallography. Single crystals suitable for X-ray analysis were formed by diffusion of diethyl ether into a chloroform solution of **1**, which yielded orange crystalline needles incorporating chloroform, **1'**. Crystallographic data are

(11) Bennett, M. A.; Huang, T.-N.; Matheson, T. W.; Smith, A. K. *Inorg. Synth.* **1982**, 21, 75.

(12) Hashimoto, S.-I.; Komeshima, N.; Koga, K. *Chem. Commun.* **1979**, 437.

summarized in Tables 2 and 3. The structure was determined from data collected with a Nonius KappaCCD at $-90\text{ }^{\circ}\text{C}$. Lorentz and polarization corrections were applied to the data. The structure was solved by direct methods (SIR92) using the teXan crystal structure analysis package, and the function minimized was $\sum w(|F_o| - |F_c|)^2$. Hydrogen atoms were placed at calculated positions before each refinement and were included in the refinement, but were not refined. The chloroform showed large thermal parameters, suggesting a possible disorder. The correct configuration for **1'** as (R_{Ru} , R_{QUINAP}) was determined by reference to the known configuration of (R)-QUINAP, by a Flack parameter of 0.0314(54) for the (R_{Ru} , R_{QUINAP}) configuration, and by refinement of the opposite hand, which gave $R_w = 0.043$ compared to $R_w = 0.040$ for the correct configuration.

Typical Catalysis Experiment. A centrifuge tube was charged with [CyRuCl(R)-QUINAP]SbF₆ (0.023 g, 0.023 mmol) and CH₂Cl₂ (1 mL). A sample of AgSbF₆ (0.007 g, 0.021 mmol) was added under a stream of N₂ followed by washing of the vessel walls with CH₂Cl₂ (1 mL). A precipitate was observed after 10 min, at which point the vessel was centrifuged and a clear orange solution removed by syringe. The catalyst solution was then added to a CH₂Cl₂ solution (1 mL) of methacrolein (0.015 g, 0.21 mmol). The resultant clear orange solution was

then cooled to $-24\text{ }^{\circ}\text{C}$ for 0.5 h, at which point precooled ($-24\text{ }^{\circ}\text{C}$) CpH (0.17 g, 2.1 mmol) was added by syringe. The reaction mixture was then allowed to stand for 12 h. Analysis of an aliquot by ¹H NMR spectroscopy indicated complete conversion of methacrolein. The addition of pentanes (15 mL) resulted in the formation of an orange precipitate, and filtration through Celite provided a clear colorless solution of the cycloadduct from which the volatiles were removed under reduced pressure.

Acknowledgment. This work was supported by a grant from the National Science Foundation.

Supporting Information Available: Tables of crystal data, positional and thermal parameters, and bond lengths and angles for (R_{Ru} , R_{QUINAP})-**1**. Plot of the variation in the mole fraction of **3**, **3'**, and **3''** with temperature. Stack plots of VT NMR spectra for **2** and the catalyst mixture of **2**, **3**, **3'**, and **3''** on addition of 10 equiv of methacrolein to compound **2**. The ¹H, ¹³C{¹H}, and ³¹P{¹H} NMR data for **1** as a 5:1 mixture of diastereomers.

OM0010767